Variability in the Solar Wind

S. T. LEPRI[1], J. RAINES, A. B. GALVIN[2], L. M. KISTLER[2], S. A. LIVI[3]

[1]THE UNIVERSITY OF MICHIGAN, CLIMATE AND SPACE SCIENCES AND ENGINEERING

[2]THE UNIVERSITY OF NEW HAMPSHIRE

[3]SOUTHWEST RESEARCH INSTITUTE

What are the sources of solar wind?

- Open fields in coronal holes
- Dipolar Streamers centered at the heliospheric current sheet which separate coronal holes of opposite polarity
- Psuedostreamers- originates in coronal holes and separates coronal holes of the same polarity. Observed in-situ, these have no embedded current sheet.
- Transients-originate in coronal mass ejections, or other bursty releases of plasma

(Owens et al., 2014, Antiochos et al. 2011, Riley and Luhmann 2012, Crooker et al. 2012)

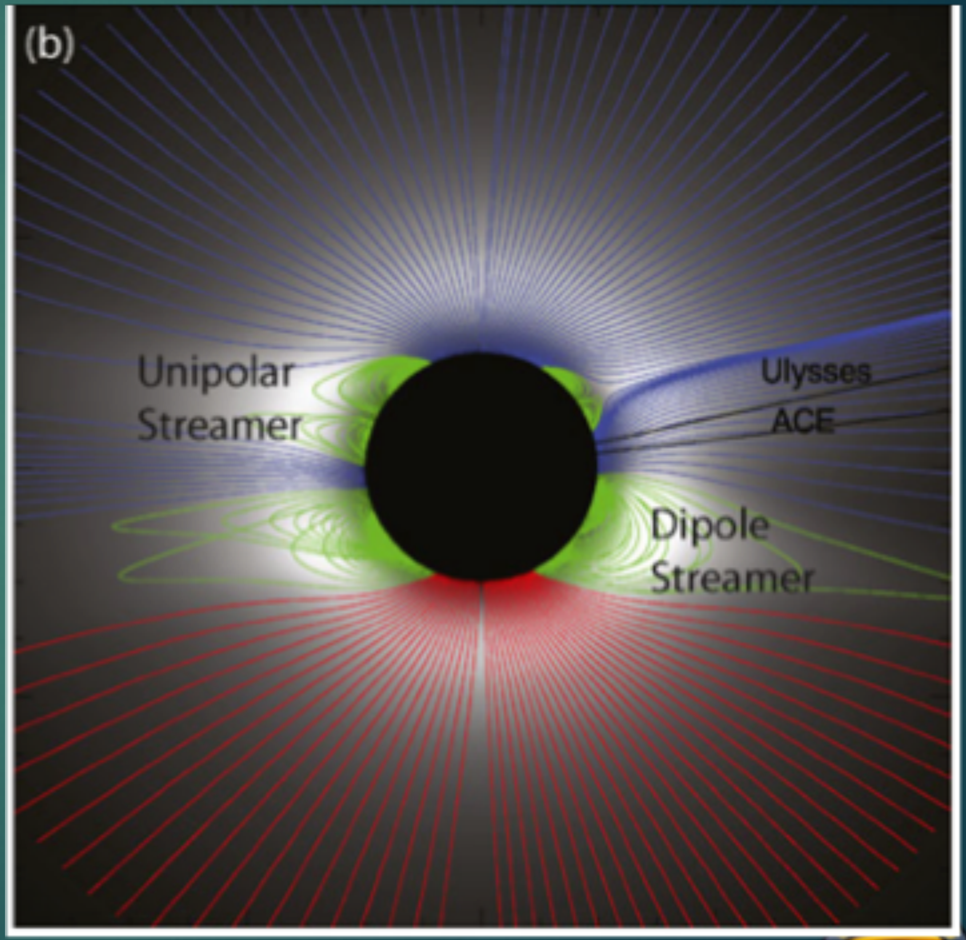

Riley and Luhmann, 2012

In determining the sources of the wind from in-situ measurements…

- "Difficulties arise because much of the solar wind at 1 AU has undergone some kind of processing or mixing…, such that the global magnetic topology and coronal connections are not easy to determine ", Cranmer et al. (2017)

Traditional Views of the Solar Wind: Separation by speed

Table 1 Properties of slow and fast solar wind streams

Cranmer et al. (2017)

Quantity	Slow wind	Fast wind
Radial flow speed	250–450 $\mathrm{km\,s^{-1}}$	450–800 $\mathrm{km\,s^{-1}}$
Proton density (1 AU)	5–20 $\mathrm{cm^{-3}}$	2–4 $\mathrm{cm^{-3}}$
Proton temperature (1 AU)	0.03–0.1 MK	0.1–0.3 MK
Electron temperature (1 AU)	0.1–0.15 MK	~0.1 MK
Freezing-in temperature (corona)	1.4–1.7 MK	1.0–1.3 MK
Helium abundance	0.5–4%	3–5%
Heavy ion abundances	low-FIP enhanced	~photospheric
Ion/proton temperature ratio	$< m_{\mathrm{ion}}/m_p$	$> m_{\mathrm{ion}}/m_p$
Coulomb collisional age (1 AU)	0.1–10	0.001–0.1
Coronal WSA expansion factor	15–100	3–10
Coronal sources (Sects. 2.2–2.3)	streamers, quiet loops, active regions, coronal hole boundaries, separatrices	coronal hole cores

What can we learn from heavy ions?

- Ion composition is determined within 4-5 R_s
  - reflects that of the source region from where the wind is accelerated (either open field coronal holes or closed loops).
  - Determined by loop properties and release mechanisms and does not evolve as it propagates through the heliosphere.
- Elemental abundances are determined within 1-2 Rs
  - Processes in the low atmosphere determine the elemental abundances.
  - Fractionation processes ongoing in the low atmosphere affect abundances.
- Solar wind composition is a key parameter for tracking heliospheric structures to their sources on the Sun
- Plasma processes may depend on M, Q and heavy ions are critical for characterizing behaviors.
- Plasma processes governing the solar wind are mediated by He, H, minor heavy ion behave like test particles in the flow

Ionization

- In the solar corona, particles undergo ionization and recombination by
  - Collisional ionization by electron impact

    $X^{i} + e \rightarrow X^{i+1} + e + e$
  - Dielectronic and Radiative recombination

    $X^{i} + e \rightarrow X^{i-1**} \rightarrow X^{i-1} + \nu$

    $X^{i} + e \rightarrow X^{i-1} + \nu$
- The source term for the creation and destruction of the ion, X^{i}, is

dn_i/dt	Source term for X^{i}
C_i	Ionization rate
$R_{xr,i}$	Recombination rate
n_i	Density of X^{i}
n_e	Density of electrons

$$\frac{dn_i}{dt} = -C_i n_i n_e - (R_{dr,i} + R_{rr,i}) n_i n_e + C_{i-1} n_{i-1} n_e + (R_{dr,i+1} + R_{rr,i+1}) n_{i+1} n_e$$

Losses due to ionization and recombination

Creation due to ionization and recombination

"Freezing-in" Concept

- Charge states of minor species are established in the inner corona by collisions with hot electrons.
- As an ion moves out of the corona, the ambient coronal electron density decreases, ion density also decreases, and collisions become so rare that
- The charge state of an ion no longer adapts itself to the ambient electron temperature by recombination, and consequently it "freezes".

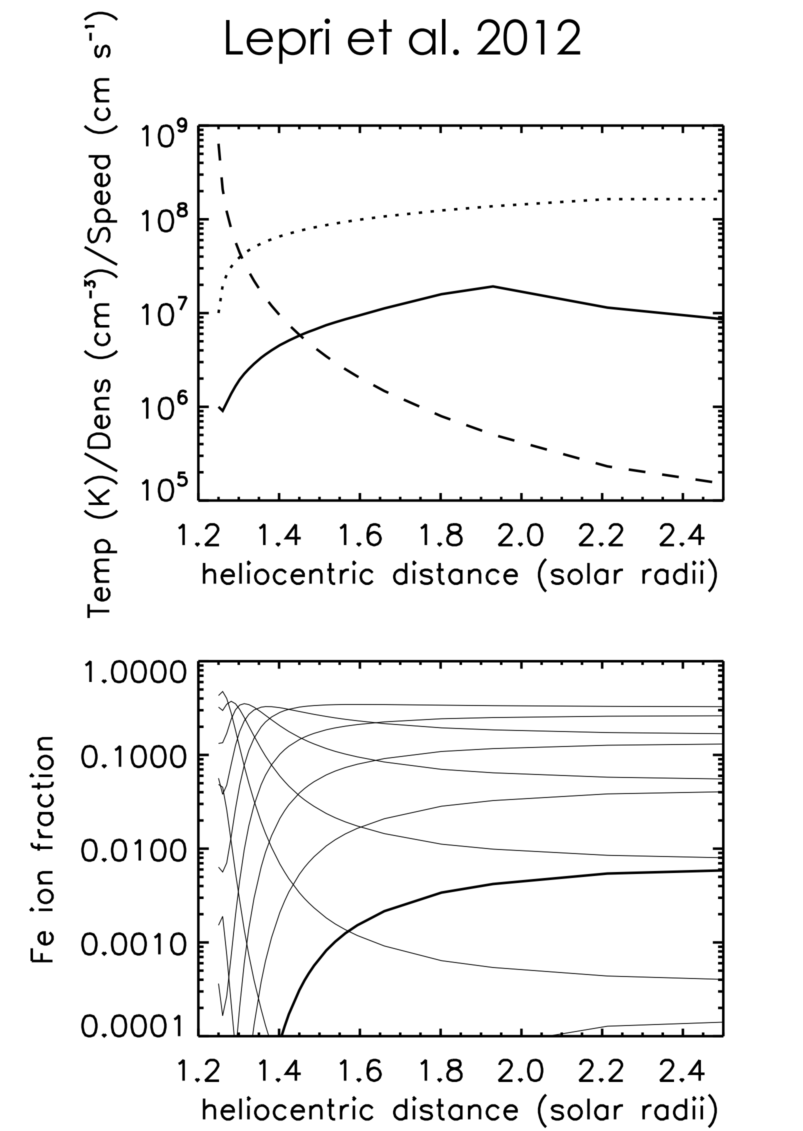

FIP Elemental Fractionation

- FIP Fractionation: Caused by the ponderomotive force and diffusion, "Ponderomotive forces are time-averaged nonlinear forces acting on media in the presence of oscillating electromagnetic fields" (Lundin and Guglielmi, 2006)
- Evaporative flow takes plasma from the chromosphere into the corona
- High wave density in the corona in closed regions draws low FIP ions up.

Lepri et al. 2012

Laming 2015

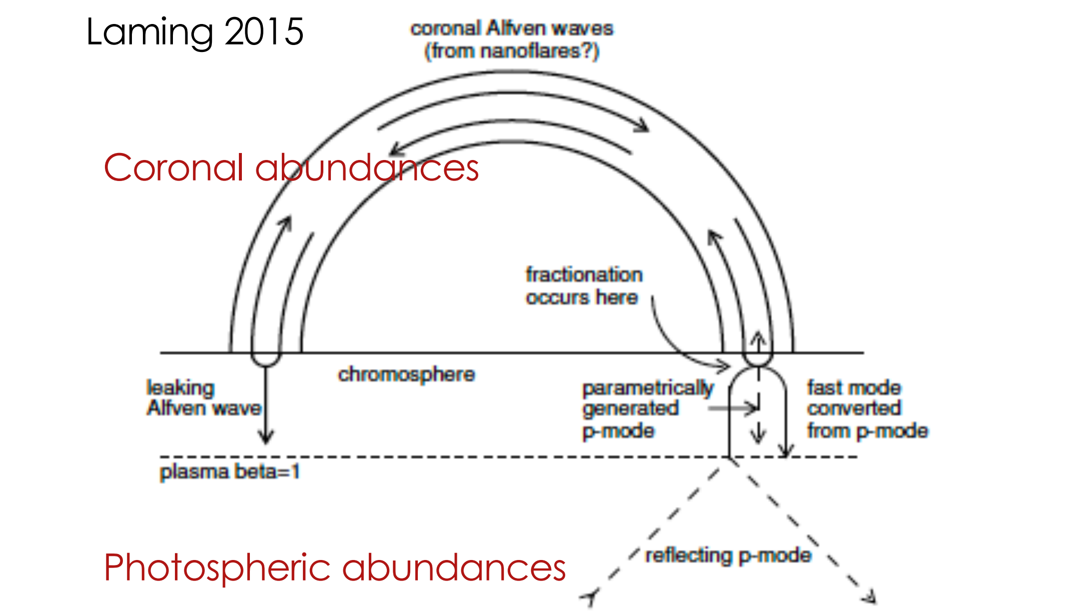

Figure 5: Schematic diagram of model loop and wave processes, adapted from Laming (2012), which follows Hollweg (1984). All footpoint wave processes may happen at both footpoints, but are here split between the two for clarity. Alfvén waves shown as thick solid lines are assumed to be generated inside the

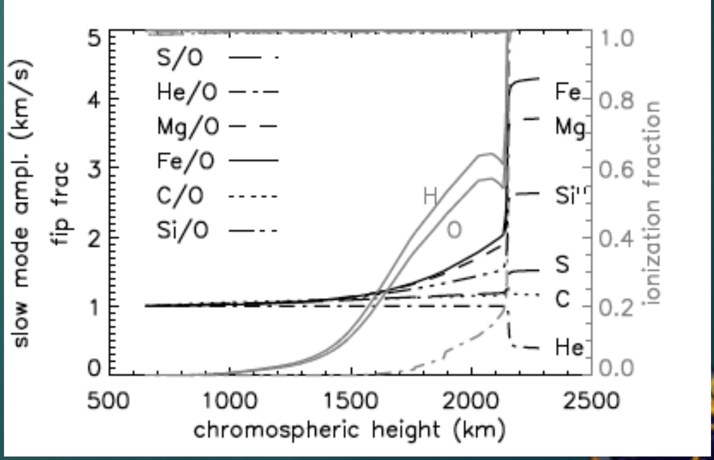

Laming 2015

Identifying Solar Wind origin by Heavy Ion Composition

- Clear anti-correlation between solar wind speed and charge states
- Fastest wind has lowest charge states and lowest Fe/O—classical fast wind (least variable?)
- Slow wind has a broader range of Fe/O (little FIP bias), but higher charge states (most variable?)

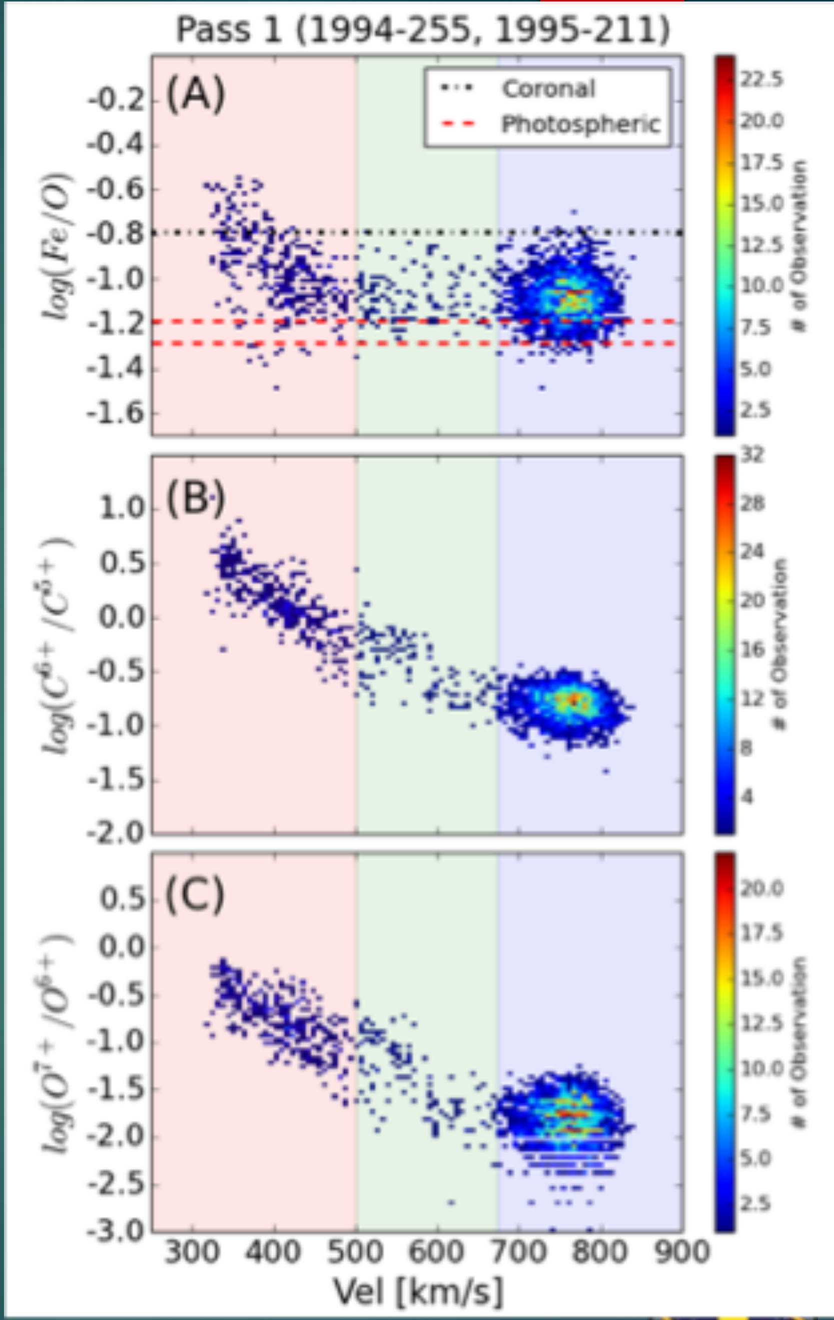

Stakhiv et al. 2015

Stakhiv et al. 2015, 2016

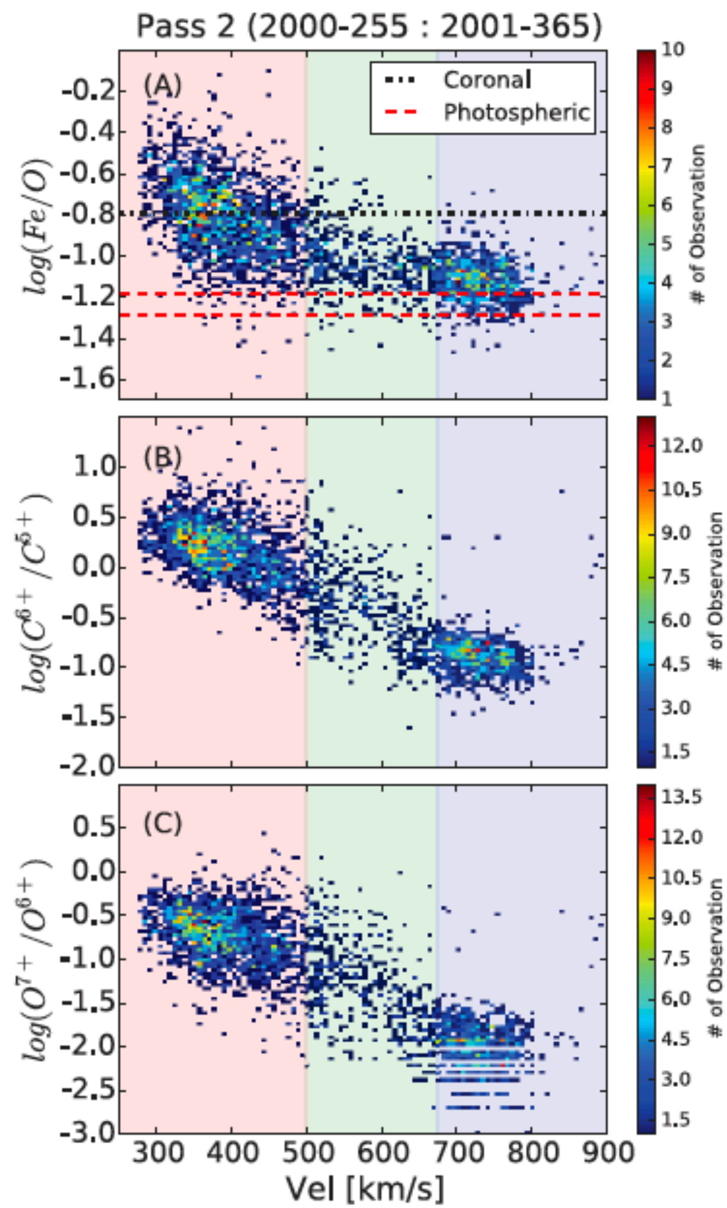

Figure 3. Compositional properties during the second Ulysses fast-latitude scan. This figure is the same as Figure 2, but occurring 6 yr later during the 2001 solar maximum. The same trends seen in Figure 2 are seen here.

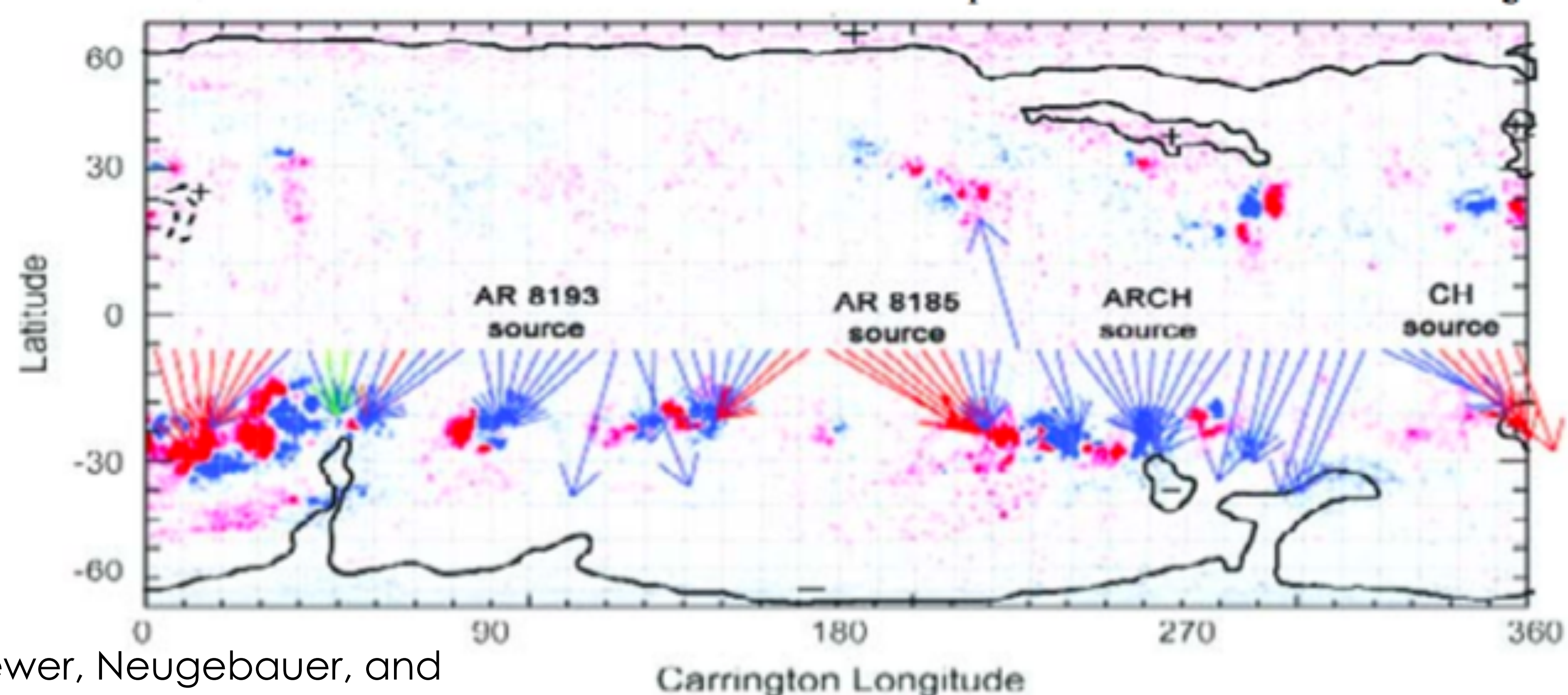

Liewer, Neugebauer, and Zurbuchen (2003)

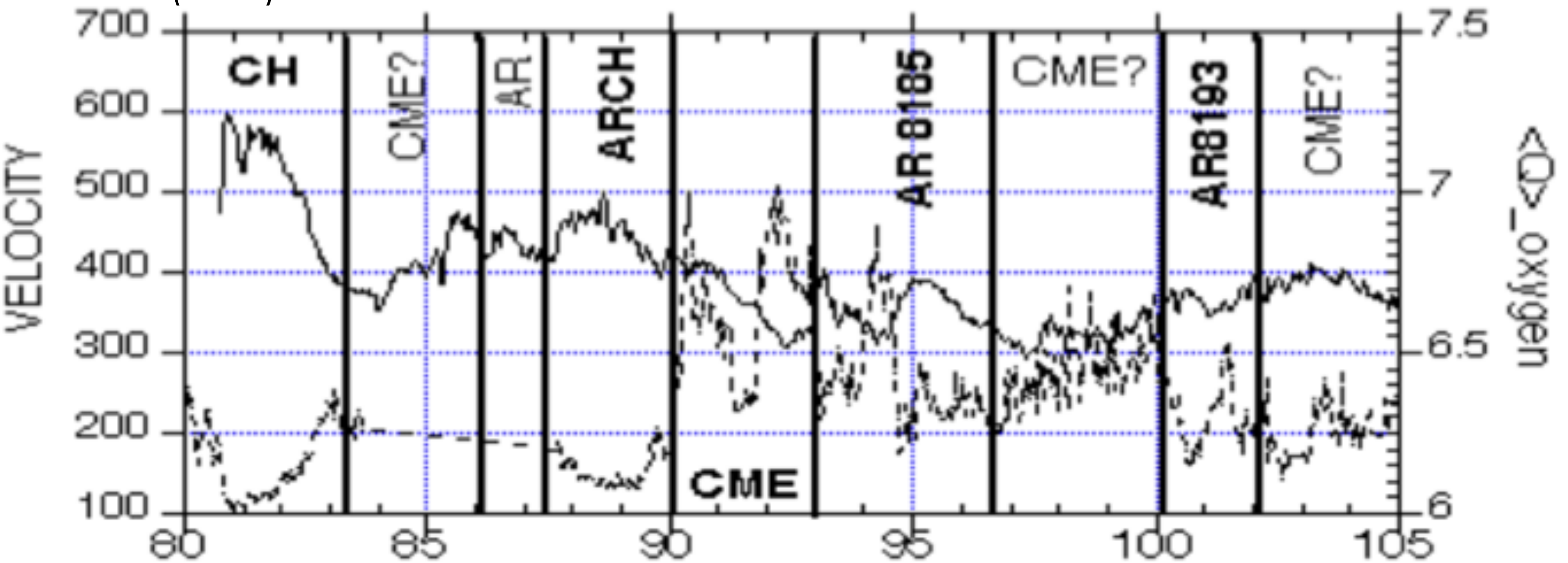

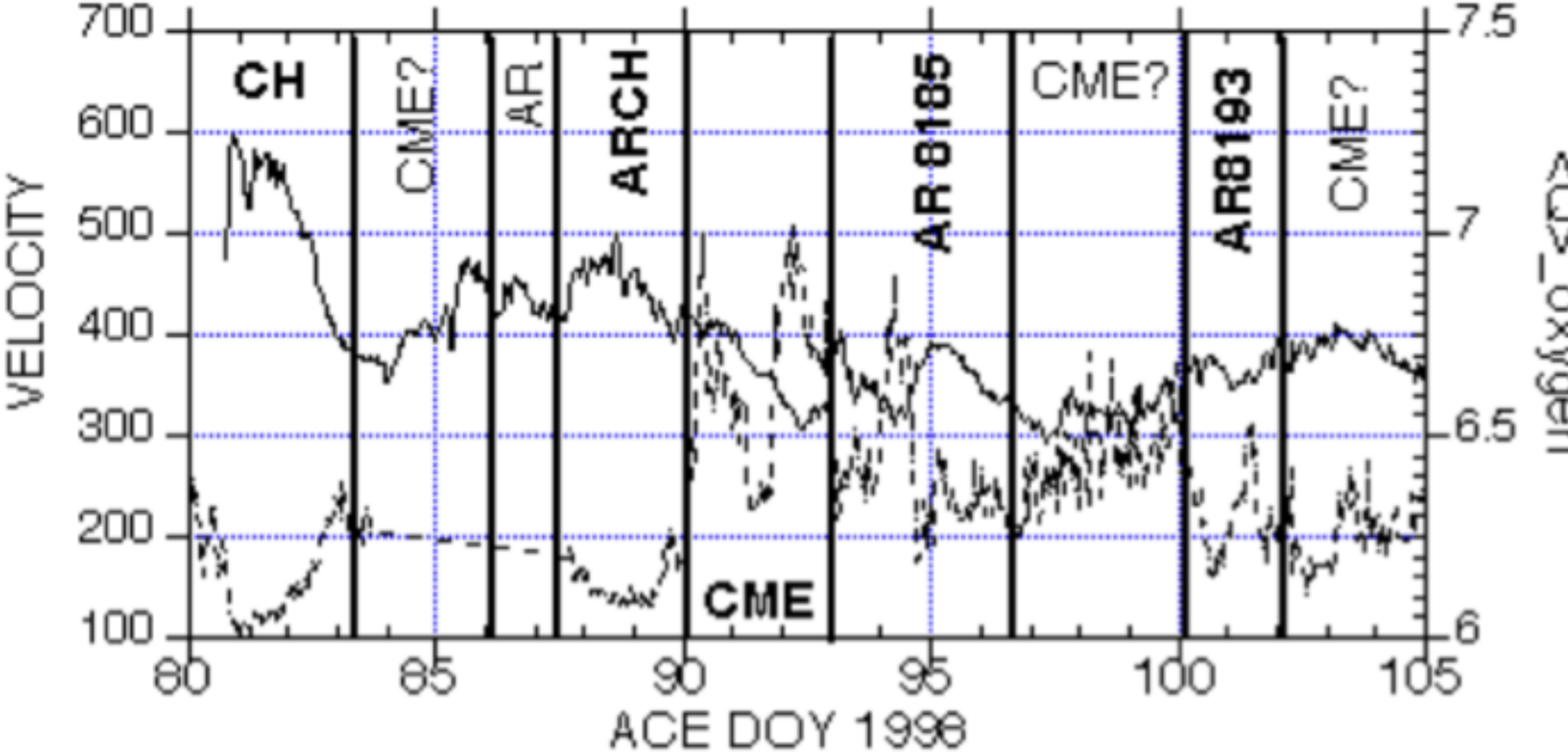

FIGURE 4. ACE solar wind proton velocity (solid) and average Oxygen charge state <Q> (dashed). The vertical lines separate wind from different sources, determined from the mapping (Figure 2). Carrington longitude goes from right to left: Day 80 maps to ~360° and Day 105 maps to 55°.

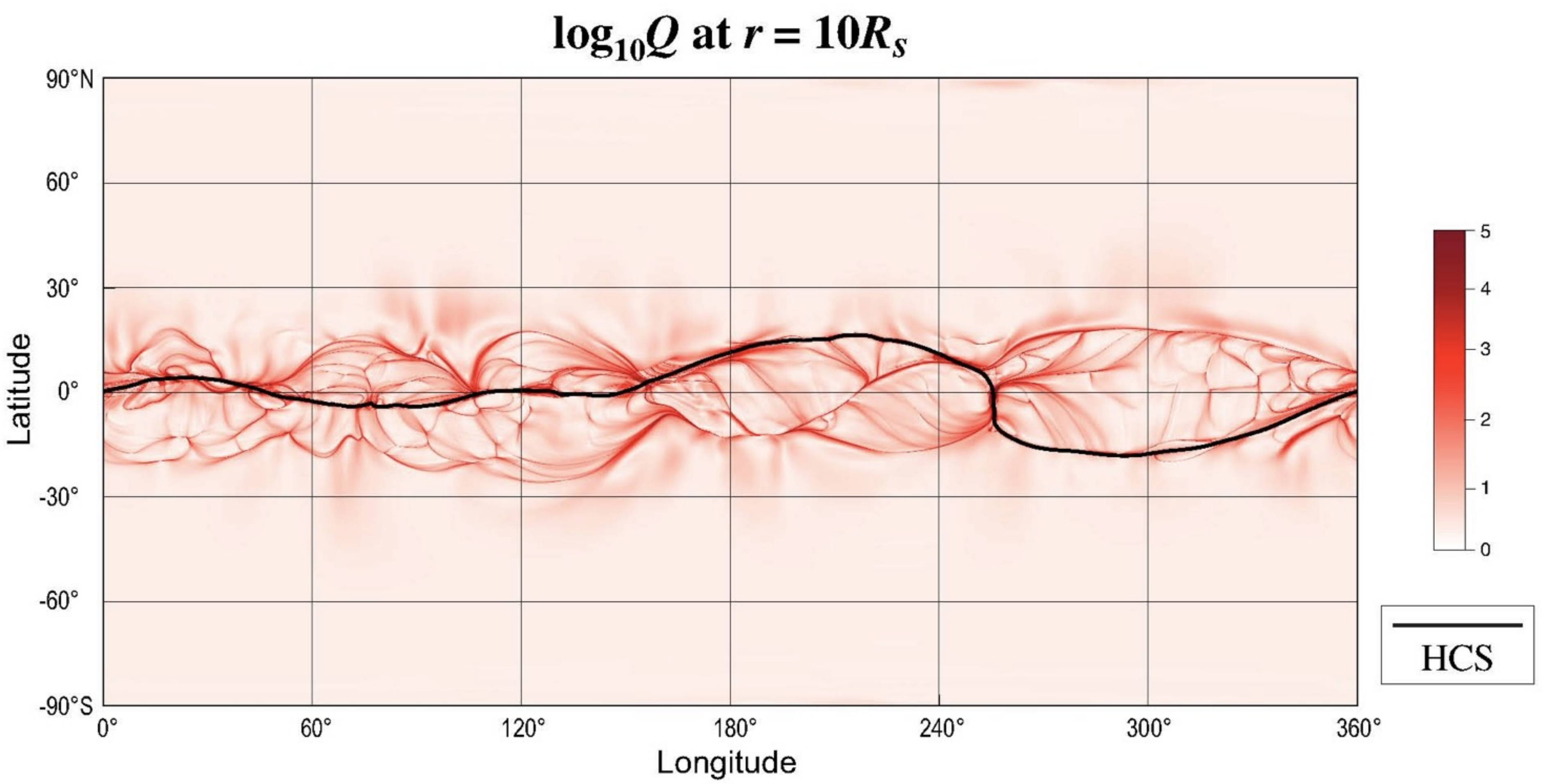
$\log_{10}Q$ at $r = 10R_s$
90°N
60°
30°
0°
-30°
-60°
-90°S
Latitude
0°
60°
120°
180°
240°
300°
360°
Longitude
5
4
3
2
1
0
HCS

Coronal electron temperatures vary significantly

- Solar wind plasma undergo heating processes and release that vary on time scales of <2 hours
- ICME structure reveals multiple plasma components with significant variation across event
- Cold material observed in ICMEs infrequently, and lasting < few hours; this is at the limit of current sensors
- Hot plasma coexists with typical solar wind type plasma at times
- Variability across the ICME can be significant at times.
- High time resolution measurements may enable further disentangling of sources of multi-temperature plasma.

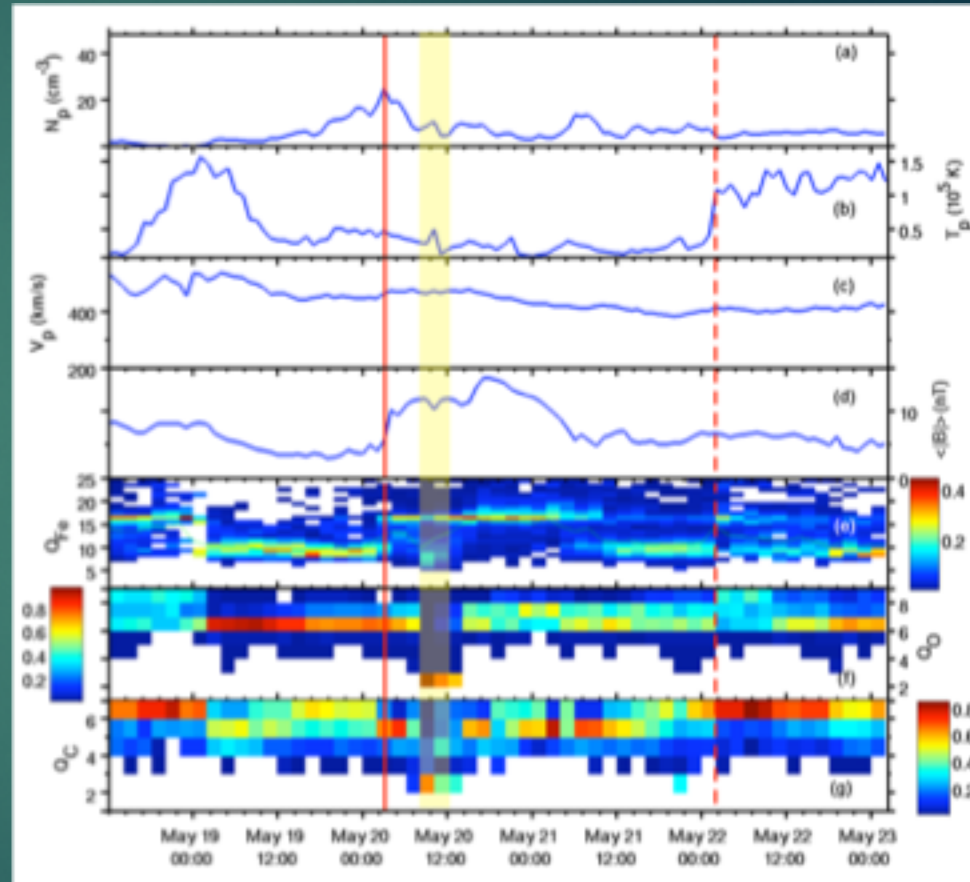

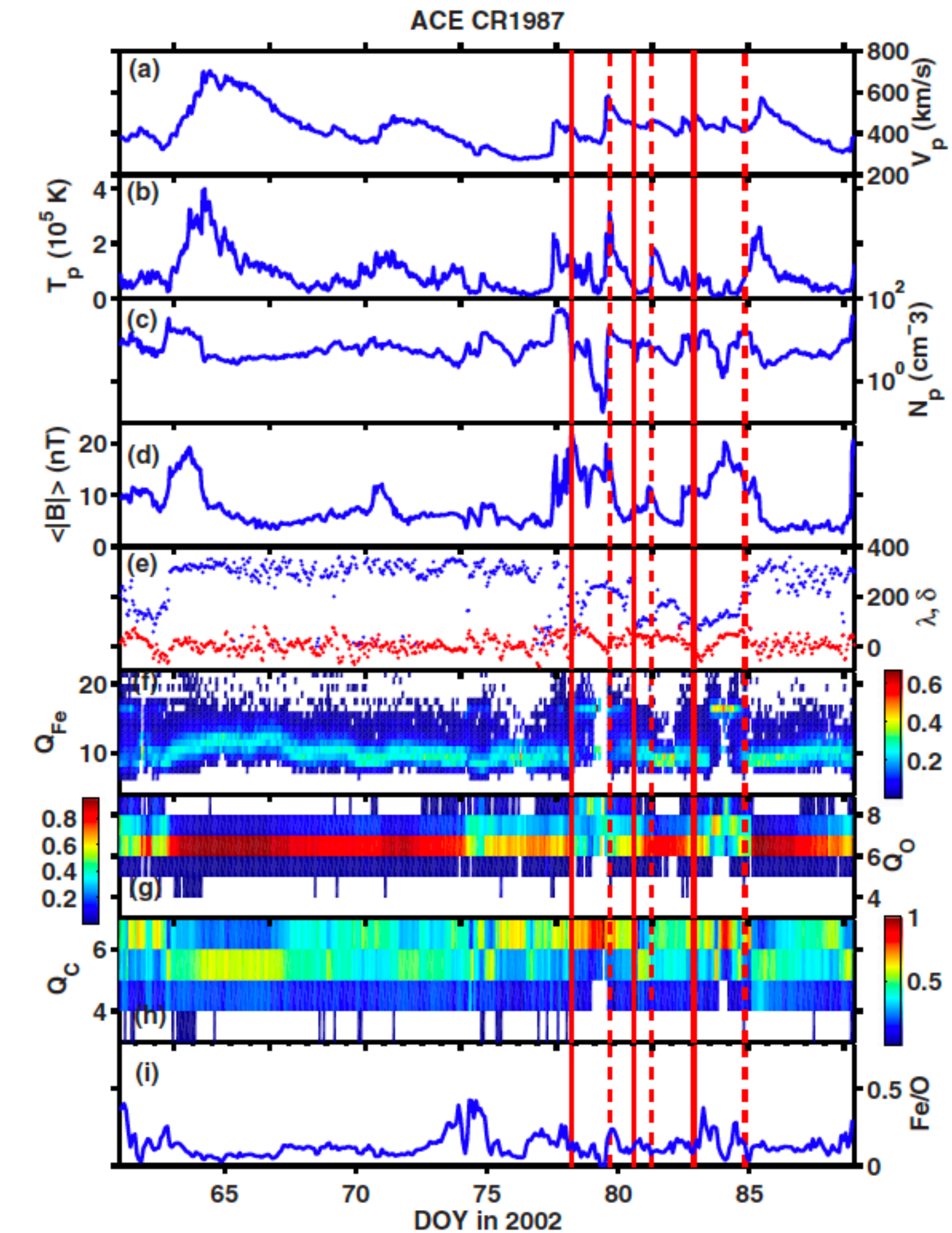

ACE CR1987
(a)
(b)
(c)
(d)
(e)
(f)
(g)
(h)
(i)
800
600
400
200
V_p (km/s)
T_p (10^5 K)
4
2
0
10^2
10^0
N_p (cm^{-3})
<|B|> (nT)
20
10
0
400
200
0
λ, δ
Q_{Fe}
20
10
0.6
0.4
0.2
0.8
0.6
0.4
0.2
8
6
4
Q_O
Q_C
6
4
1
0.5
0.5
0
Fe/O
65
70
75
80
85
DOY in 2002

Effects of photoionization on Solar Wind Charge States

The Astrophysical Journal Letters, 812:L28 (6pp), 2015 October 20

Landi and Lepri (2015)

Landi & Lepri

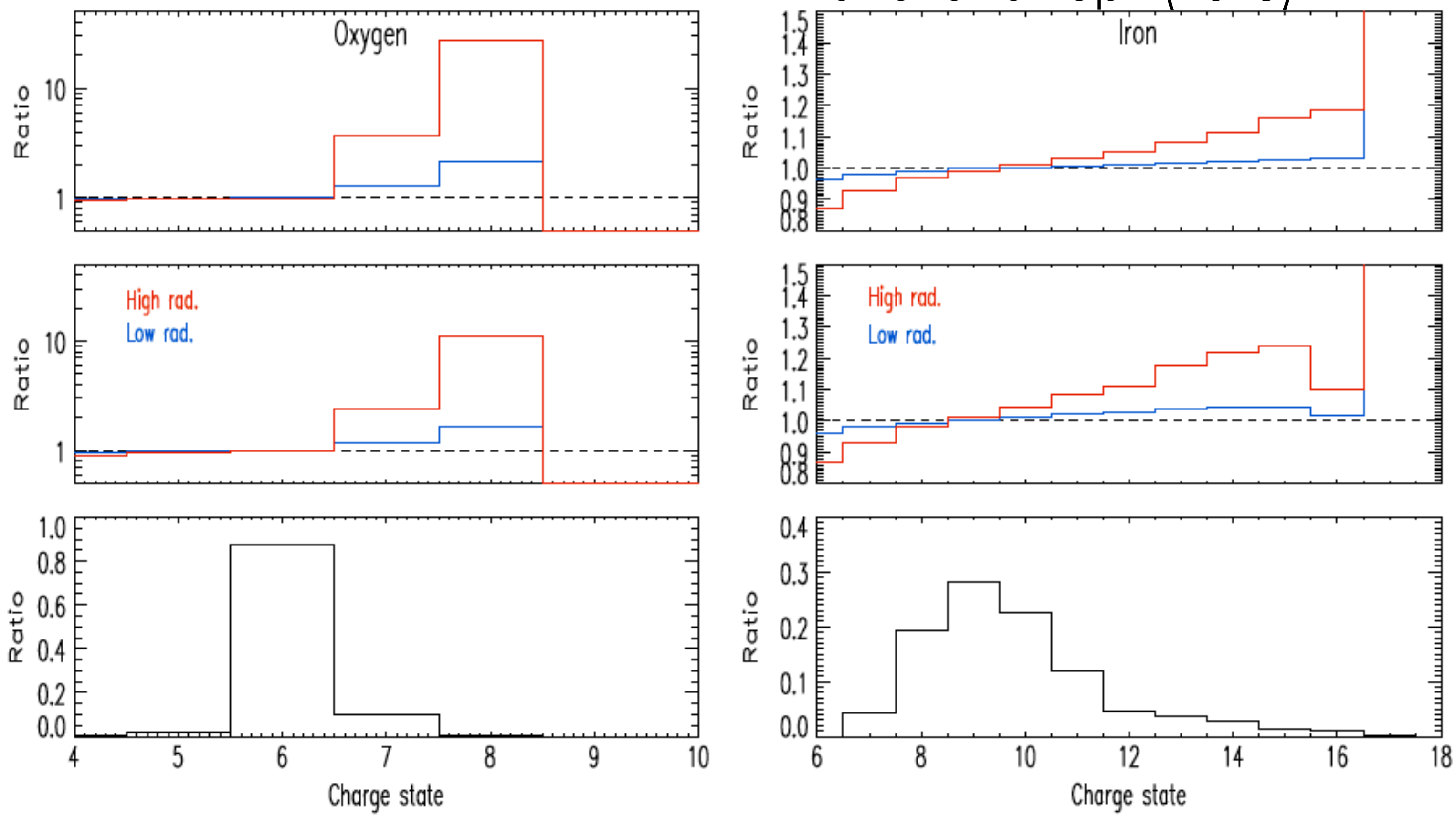

Figure 2. Left: ratio between the oxygen frozen-in charge states calculated with photoionization, to those calculated without it. Red and blue curves correspond to ionizing radiation from solar maximum and minimum, respectively. The top panel is the fast wind, the middle panel is the slow wind, and the bottom panel is the average wind charge state distribution. Right: same as left panels, for iron. The ratio for ions Fe^{17+} and higher is larger than 1.5.

Reconnection as a release process of the solar wind

- Quasi-periodic structures have been observed in the solar wind
  - ~90 min in Kepko et al. 2016
  - ~5 hrs, 20 hrs in Edmondson et al. 2013
- These have been interpreted as associated with interchange reconnection
- Smaller time scale studies and characterization have been hampered by lack of data at time scales <12 min.
- Observations closer to the Sun may reveal cleaner peaks/signatures of reconnection

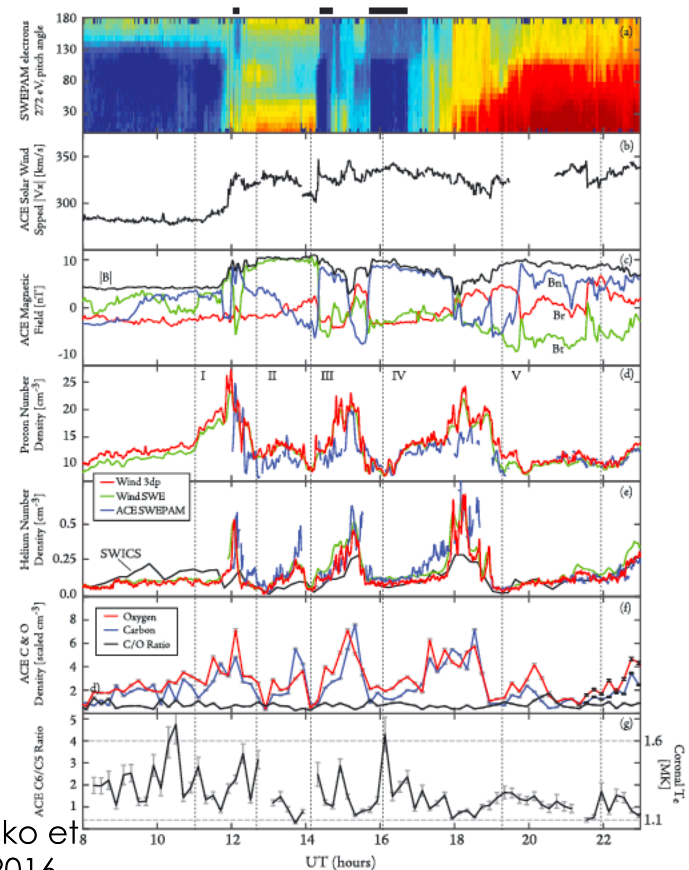

Kepko et al. 2016

Figure 1. In situ observations of the periodic density structures (labeled I–V) observed by the ACE and Wind spacecraft near 1 AU on 15 June 1999. Plotted are (a) 272 eV electron pitch angles from ACE SWEPAM; (b) ACE solar wind velocity, $|V_x|$; (c) ACE magnetic field observations in RTN coordinates; (d) proton number density from ACE and Wind; (e) helium number density from ACE and Wind; (f) oxygen ($\times 1 \times 10^{-3}$) and carbon ($\times 2 \times 10^{-3}$) number densities and C/O ratio; (g) the C^{6+}/C^{5+} ratio measured by ACE SWICS. Ratio values of 4 are equivalent to 100% C^{6+}, within the resolution of the measurements. Error bars shown for ACE SWICS data in Figures 1f and 1g represent the statistical uncertainty and are on average less than 10% for the abundances and ~30% for the charge state ratio. Data with relative errors greater than 50% have been neglected in the analysis. Horizontal lines show inferred coronal temperature T_e. Black bars at the top of the figure indicate times of magnetic disconnection from the Sun, as inferred by the electron heat flux data.

Extreme enhancements of low FIP ions

- Period of extreme (>8 times the photospheric abundances) enhancements of low FIP ions are observed during the ACE mission with SWICS.
- Enhancement factors of >20 are observed during the mission, although the highest enhancement factors are observed infrequently.
- There is a weak correlation with occurring during ICMEs, and this needs to be investigated further.
- Most events are short lived, lasting only a few hours. Is this due to source variability in time or space? Perhaps connections to different loops?

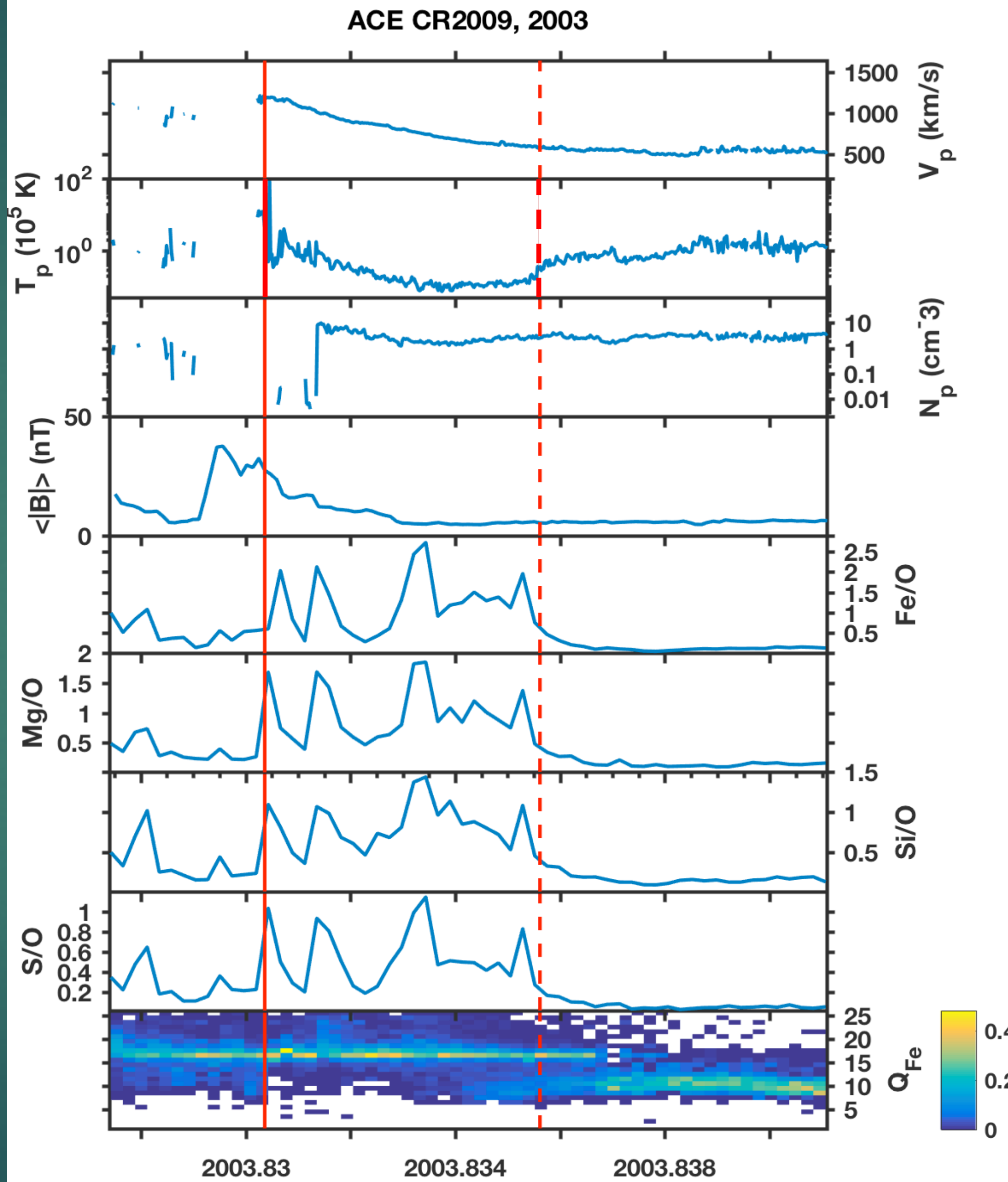

Significant Power Structure

- O^{7+}/O^{6+} composition ratio at 12-minute cadence.
- 80% significance against null-hypothesis that a given structure is due to filler signal (linear interpolation), or interference.

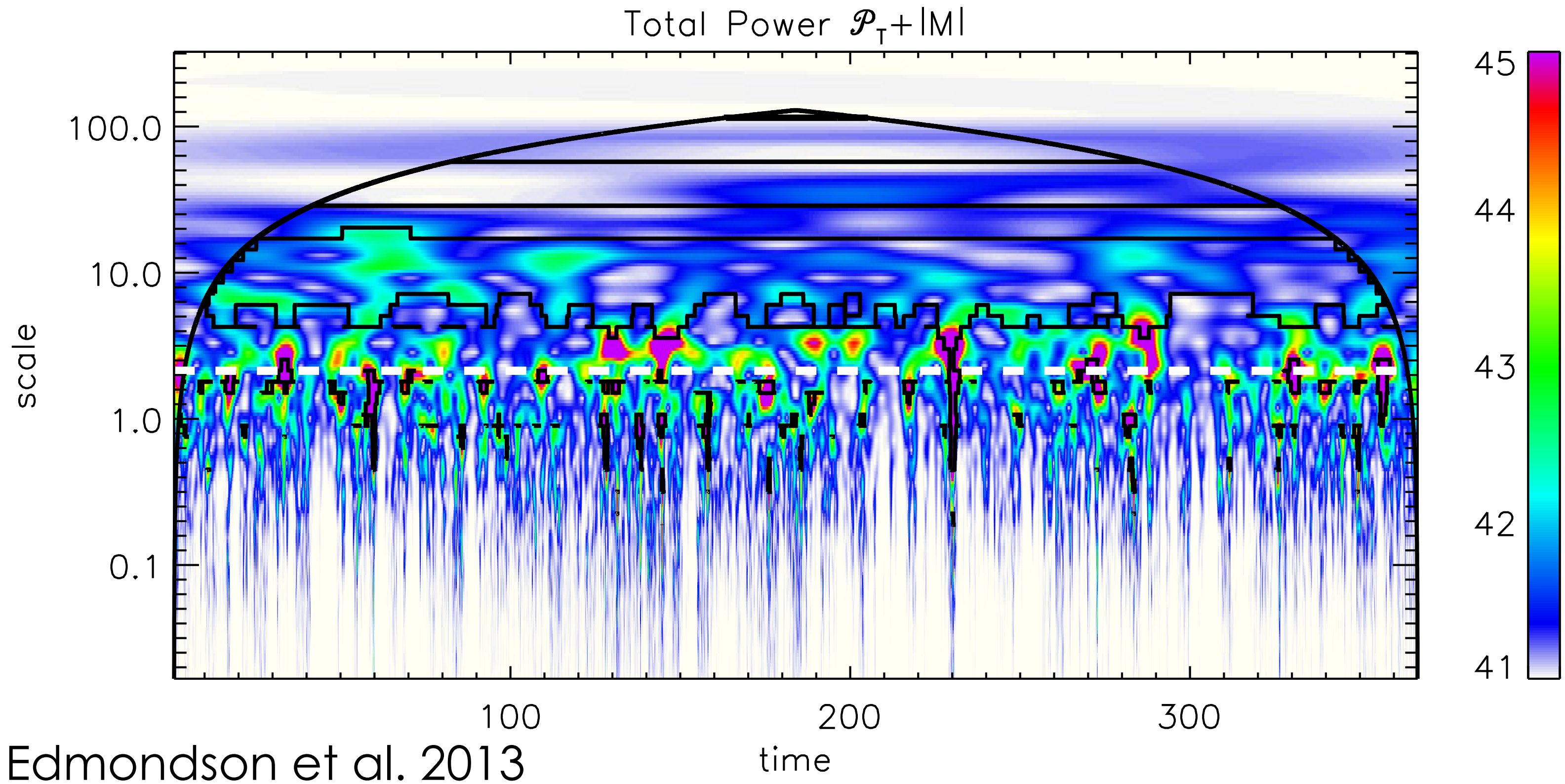

Edmondson et al. 2013

Local "Coherency" (By Wind Type)

- PDF of 2D maxima distribution by time scale.
- Small-scale coherency rates
  - 24 mins, 45 – 60 mins, 75 – 87 mins, 4 hours, 7 – 12 hours
- Large-Scale coherency rates
  - 3 – 5 days, 8 – 15 days
  - Consistent with global frequencies
- Evidence of complex magnetic field structure?

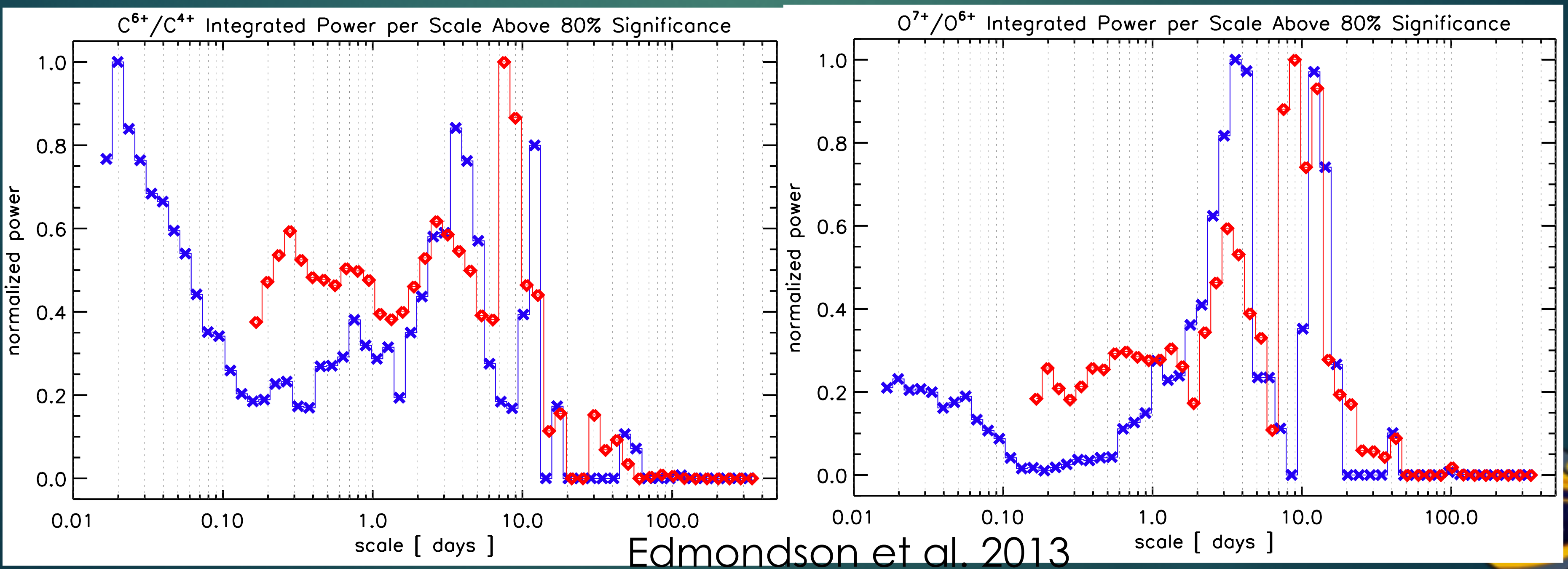

Edmondson et al. 2013

Heating of Heavy Ions at Shocks

- For quasi-perpendicular shocks, heating of heavy ions increases with increasing M/Q.
- Quasi-perpendicular shocks heated more efficiently than quasi-parallel shocks.
- This study was limited partly because SWICS observed only the radial distribution function and the minimum time resolution for heavy ions (C, O, Fe) is ~1 hour.
- 3D VDFs and 30 second time resolution will expand our opportunities to investigate shocks.

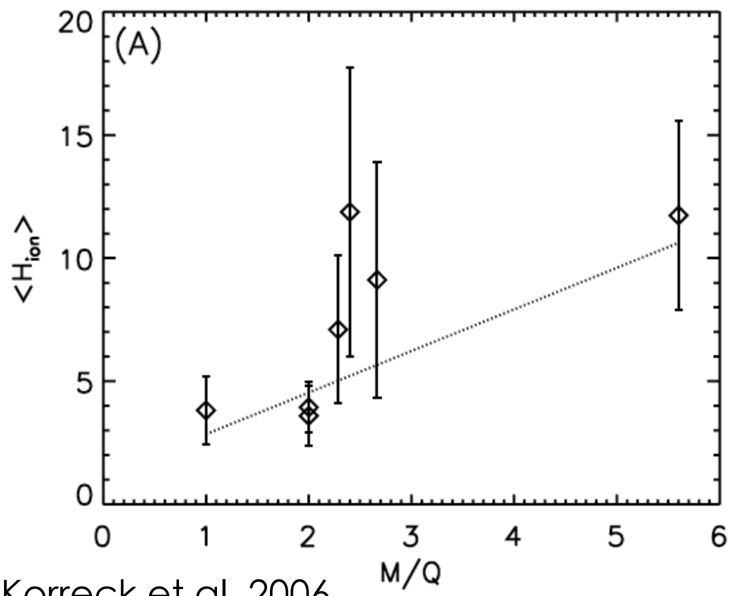

Korreck et al. 2006

$$H = \frac{v_{\mathrm{th}_d}^2}{v_{\mathrm{th}_u}^2} = \frac{3kT_{s,d}/m_s}{3kT_{s,u}/m_s} = \frac{T_{s,d}}{T_{s,u}},$$

Heating of Heavy Ions in Reconnection

- Heating of heavy ions due to reconnection in heliosphere
  - Most features are on the order of minutes to an hour
  - High Time Resolution will enable further study
  - 3D distributions will allow further characterization of heating.

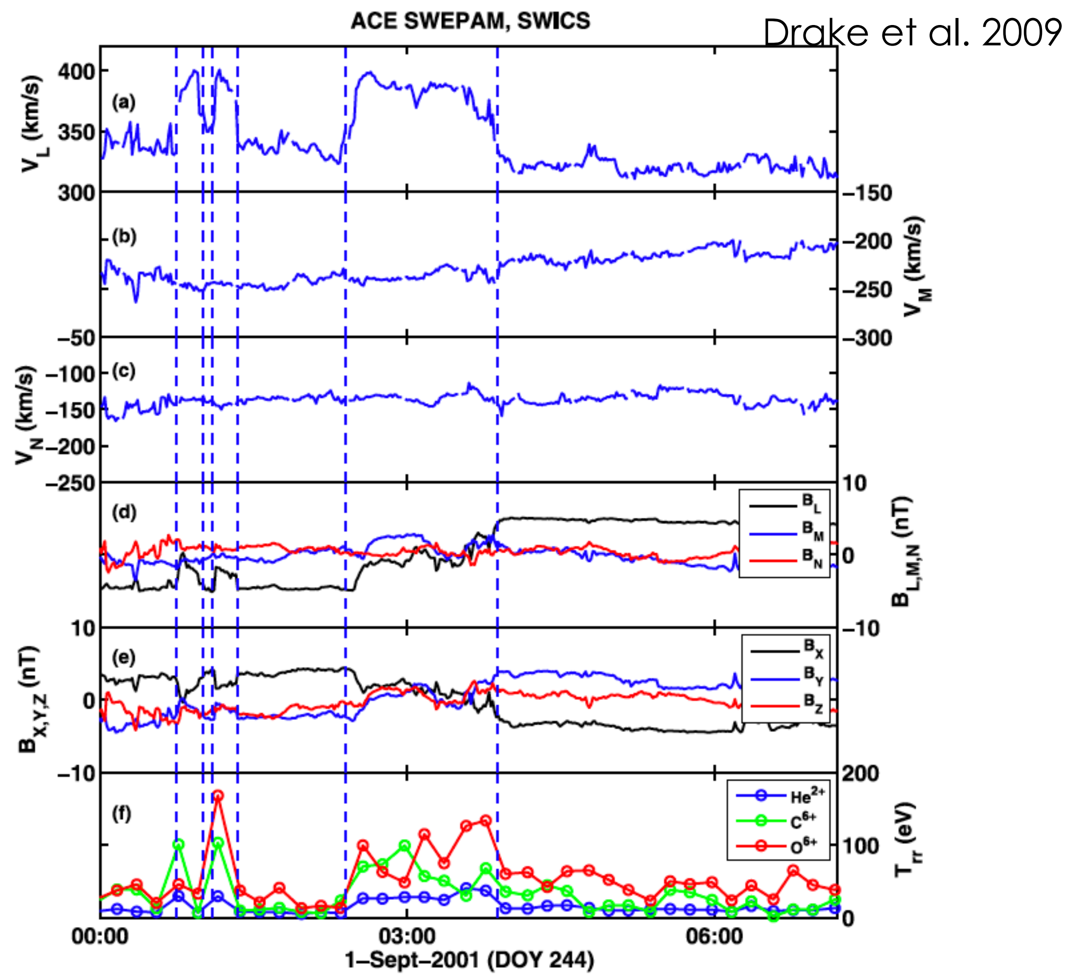

Figure 7. The time dependence of the velocities v_{LMN} and magnetic fields B_{LMN} in minimum variance coordinates; the magnetic fields in GSE coordinates; and the He^{2+}, C^{6+}, and O^{6+} radial temperatures T_{rr} from an ACE spacecraft encounter with a large-scale exhaust during reconnection in the heliospheric current sheet [*Gosling*, 2007].

Differentiating Fast and Slow by delta v

2018

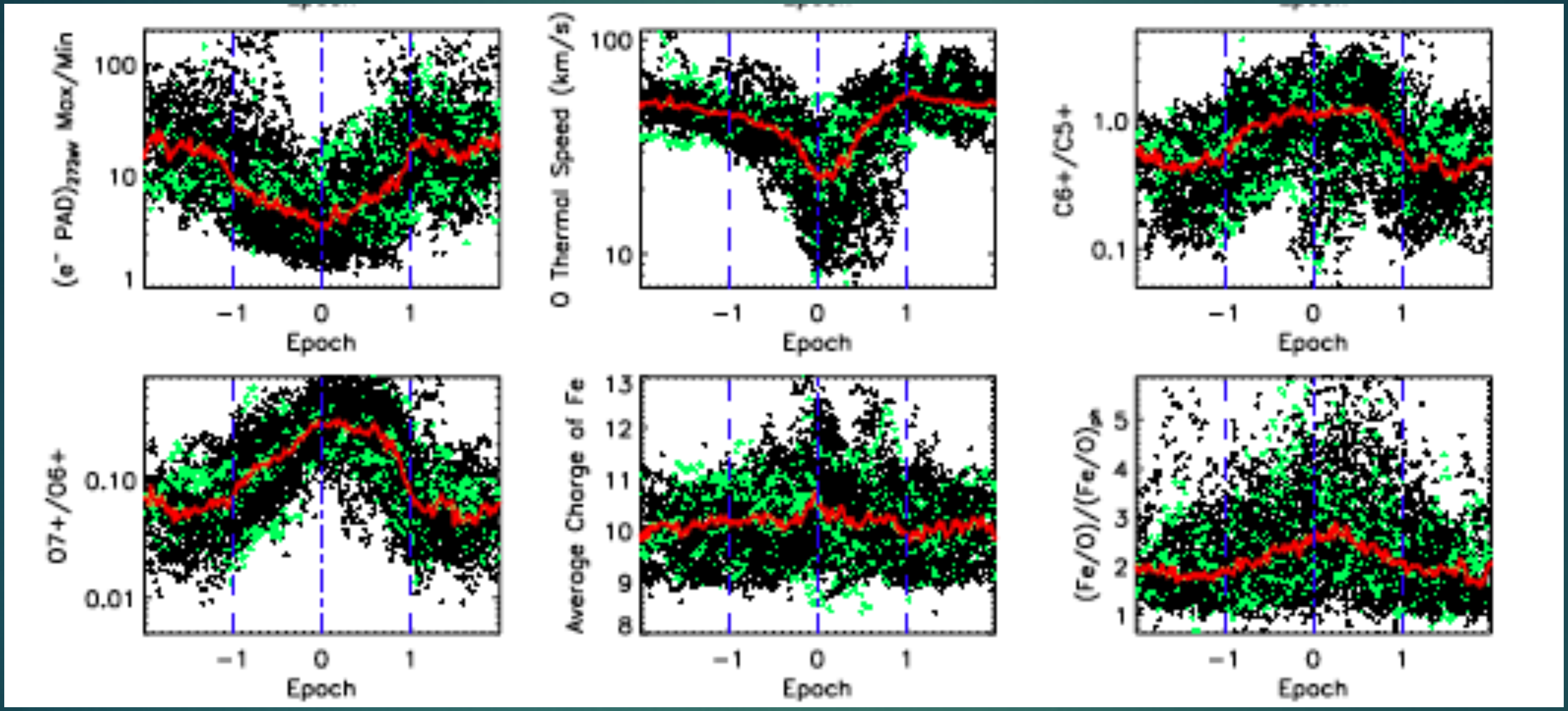

Blue: Δv>10km/s Fast to slow
Green: Δv< 10km/s to min Δv
Red: min Δv to Δv>10km/s
Black, Δv>10km/s to Slow to fast

KO ET AL. 2018

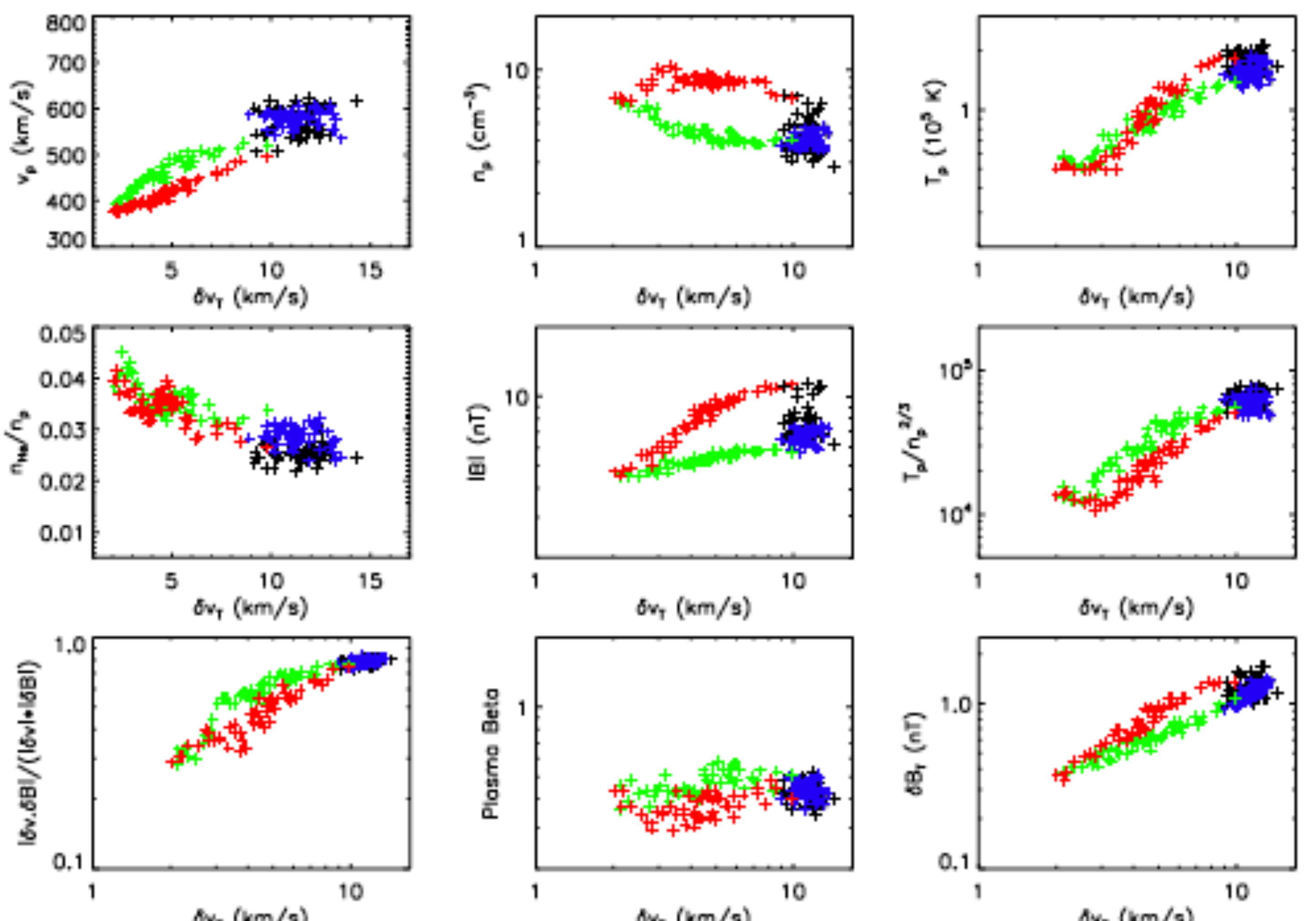

Blue: Δv>10km/s Fast to slow
Green: Δv< 10km/s to min Δv
Red: min Δv to Δv>10km/s
Black, Δv>10km/s to Slow to fast

- Where Δv is between 5-10 km/s, this is the "boundary wind" which is slow,
- At Δv<5km/s, this is the slow solar wind from inside the helmet streamer, and thus possibly linked to active regions

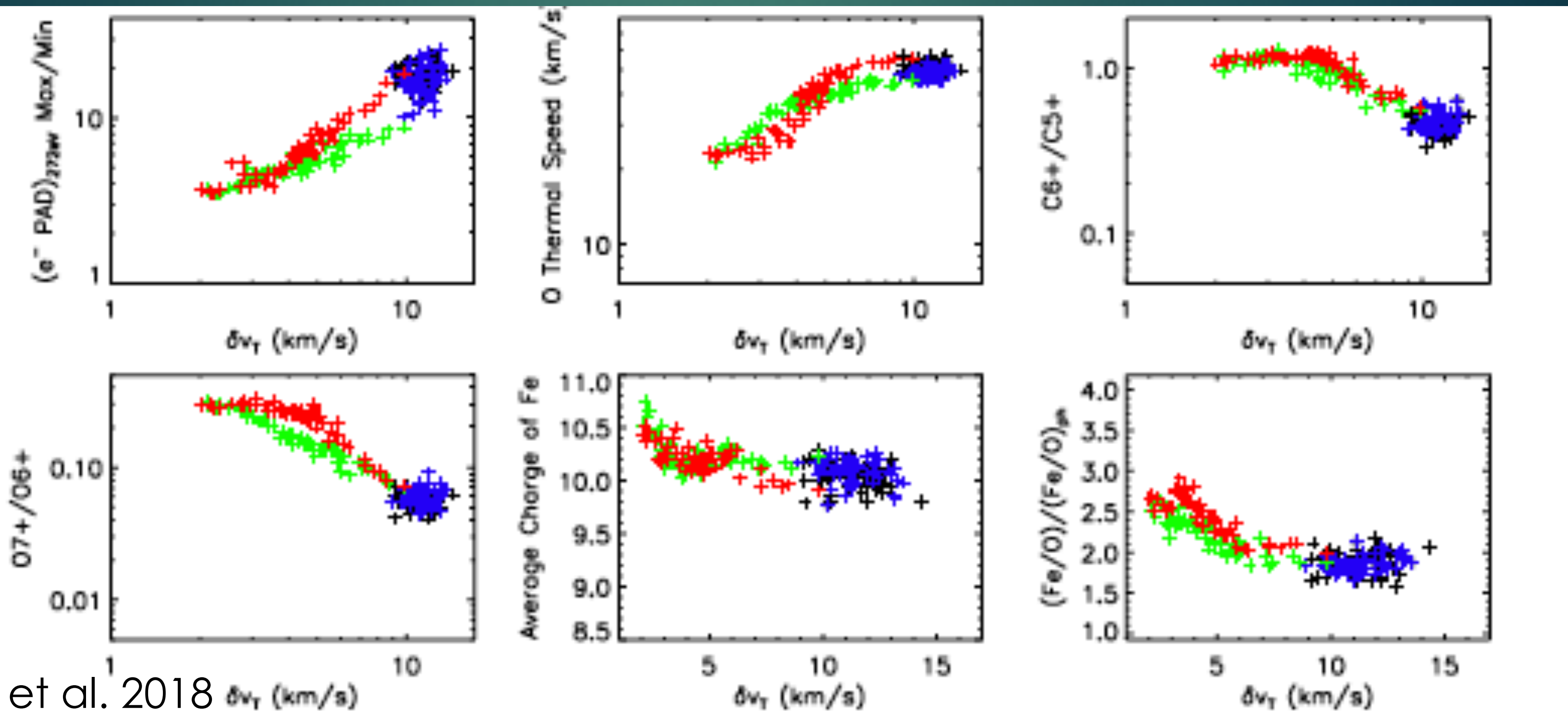

Ko et al. 2018

New Measurements from Solar Orbiter

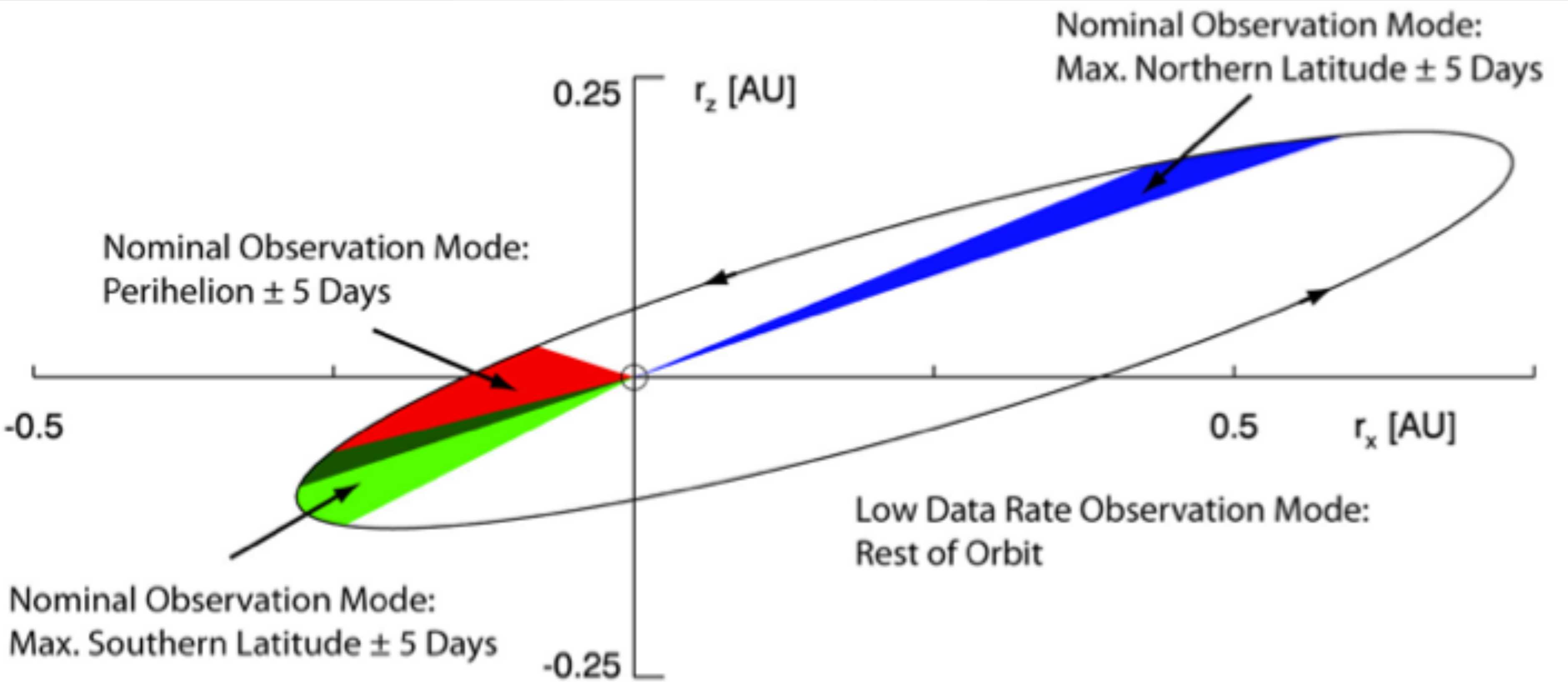

The Solar Wind Analyzer Suite

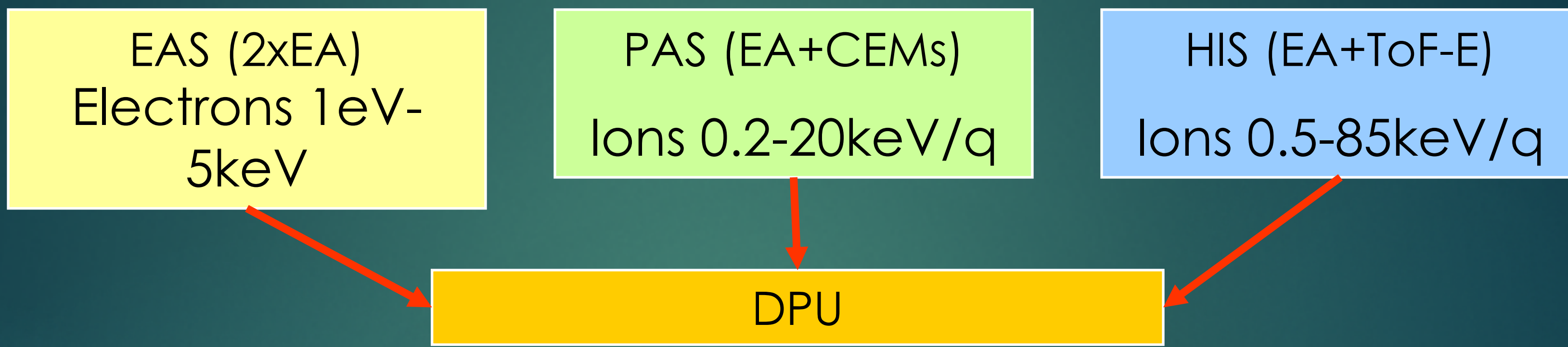

- 3D-distributions of electrons, protons and alphas
- Fast moment acquisition under all solar wind conditions
- Mass composition (FIP) and charge state (freezing T_e) of major ion constituents

Our approach:

- The Electron Analyser System (EAS, 2 sensors) will make high temporal resolution measurements of the core, halo and ‘strahl’ electron VDFs;
- The Proton-alpha sensor (PAS) will measure the VDFs of major ion species and plasma moments at high time resolution;
- The Heavy Ion Sensor (HIS) will measure the 3-D VDFs and determine the abundance and charge states of prominent minor ion species.

The scientific performance of the SWA sensors is summarised in the table below.

Parameter	Range/resolution	EAS	PAS	HIS
Sensors		2 x EA	1 x EA	1 x EA, 1 x TOF-SSD
Mass	Species	Electrons	H, He	^{3}He – Fe
	Resolution ($m/\Delta m$)	-	-	5
Energy	Range	1 eV – 5 keV	0.2 – 20 keV/q	0.5 – 60 keV/q (Az) 0.5 – 16 keV/q (El)
	Resolution ($\Delta E/E$)	12%	5 %	5.6%
	Analyzer constant (eV/V)	6.2	15.6	15.6
Angle	Range (AZ)	360°	-24° - +42° - EA	-30° - +66°
	Range (EL)	±45°	±22.5° - EA	-17° +22.5°
	Range scan (EL)	16 steps	9 steps	6 steps
	Pixel Field of view	11.25° x 3° - 8°	6° x 5°	6° x 6°
Temporal	Resolution – Normal mode	4 s moments 100 s full 3D vdfs	4 s	300sec (Heavy ions) 30 seconds (alphas)
	Burst mode	0.125 s	1/54 s	30 s (heavy ions) 4 s (alphas)
Geometric factor	Per pixel (cm^2 sr eV/eV)	Variable, $< 6.0 \times 10^{-5}$	4.6 x 10-6 cm^2 sr eV/eV	Variable, $<2 \times 10^{-5}$

SO/HIS

- Measures the composition, velocity distribution functions, and dynamic properties of solar wind heavy ions
- Measurement of 3D velocity distribution functions requires:
  - Mass,
  - Charge,
  - Energy, and
  - Direction
- Electrostatic analyzer with ion steering at entrance Followed by a time-of-flight/energy telescope with

Ion Group	Species
0	He^{2+}
1	C^{4+} to C^{6+}, O^{5+} to O^{8+}
2	Fe^{6+} to Fe^{20+}
3	Mg^{6+} to Mg^{12+}, Ne^{6+} to Ne^{9+}, Si^{6+} to Si^{12+}, etc.
4	Pick up He^{+}, $3He^{+}$
5	Single charged ions (C^{+}, O^{+}, etc.)
6	Suprathermal H^{+}, $3He^{+}$, He^{2+} and heavies

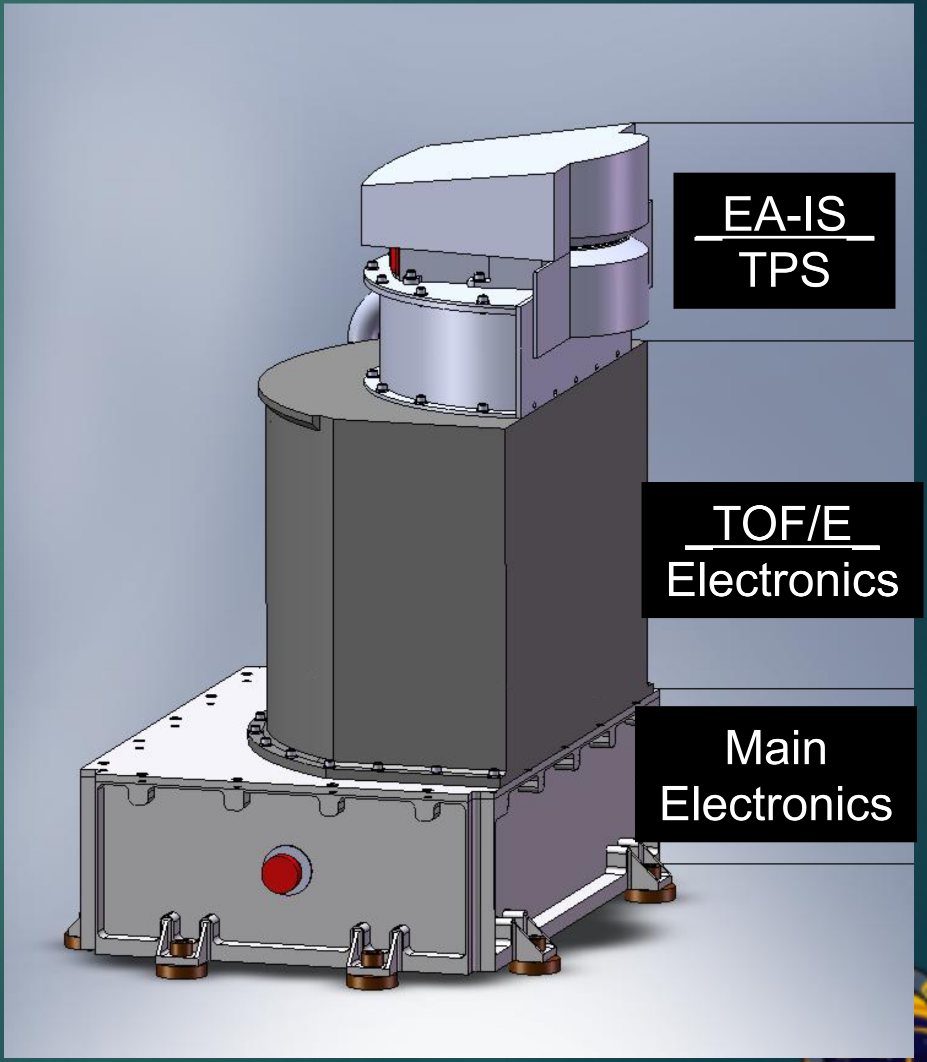

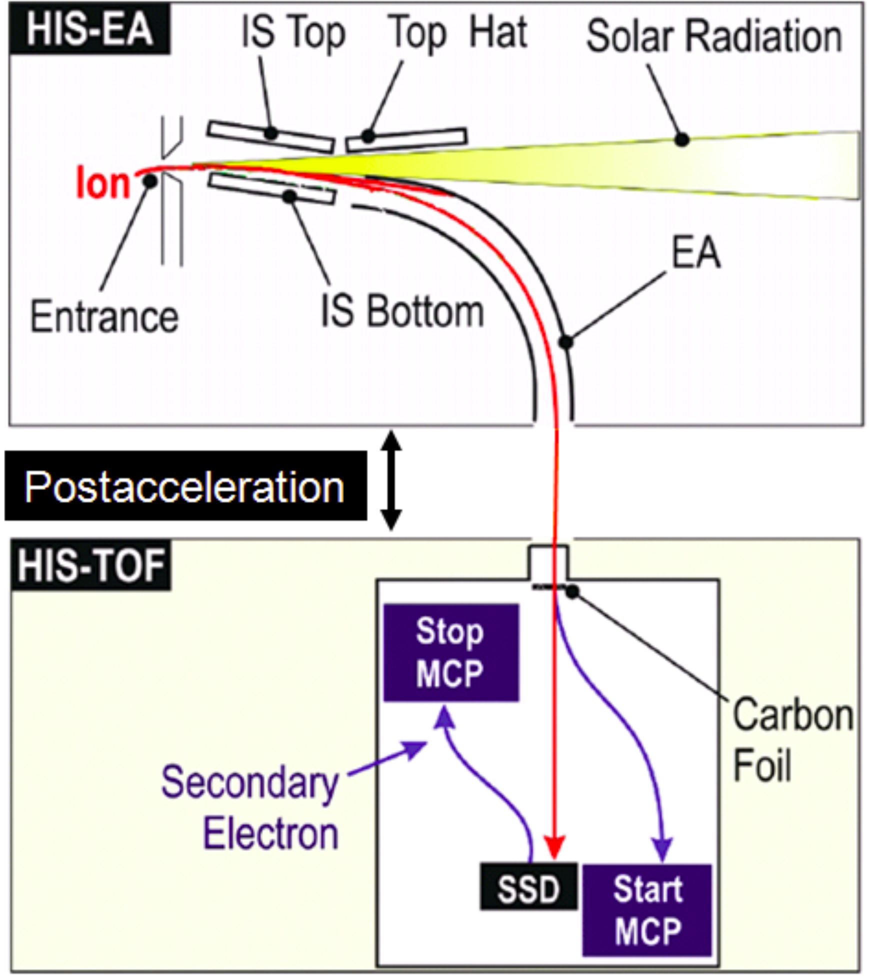

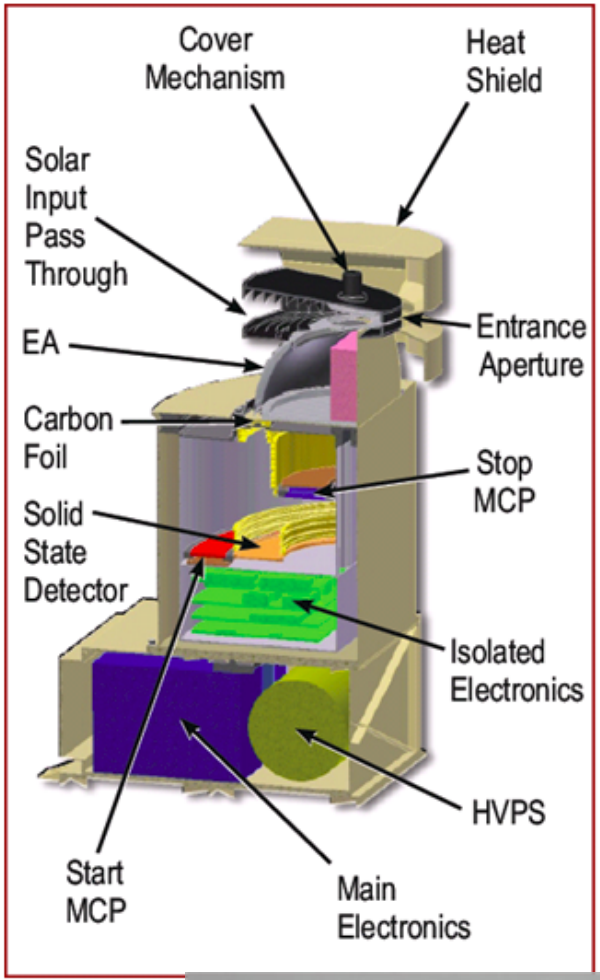

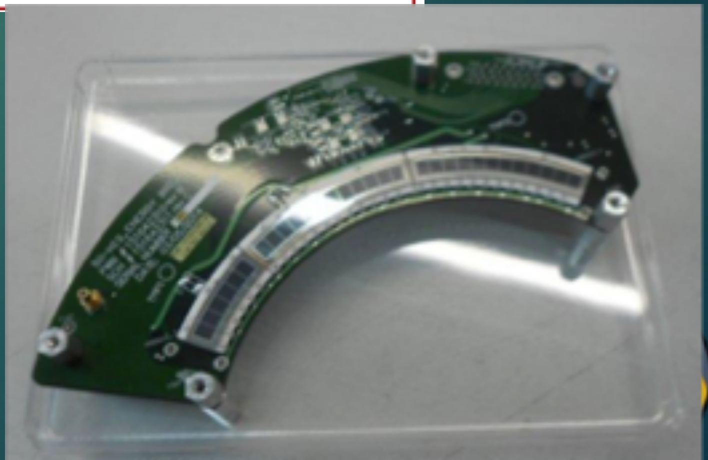

S. T. Lepri 2018 ISSI

Calibration Results

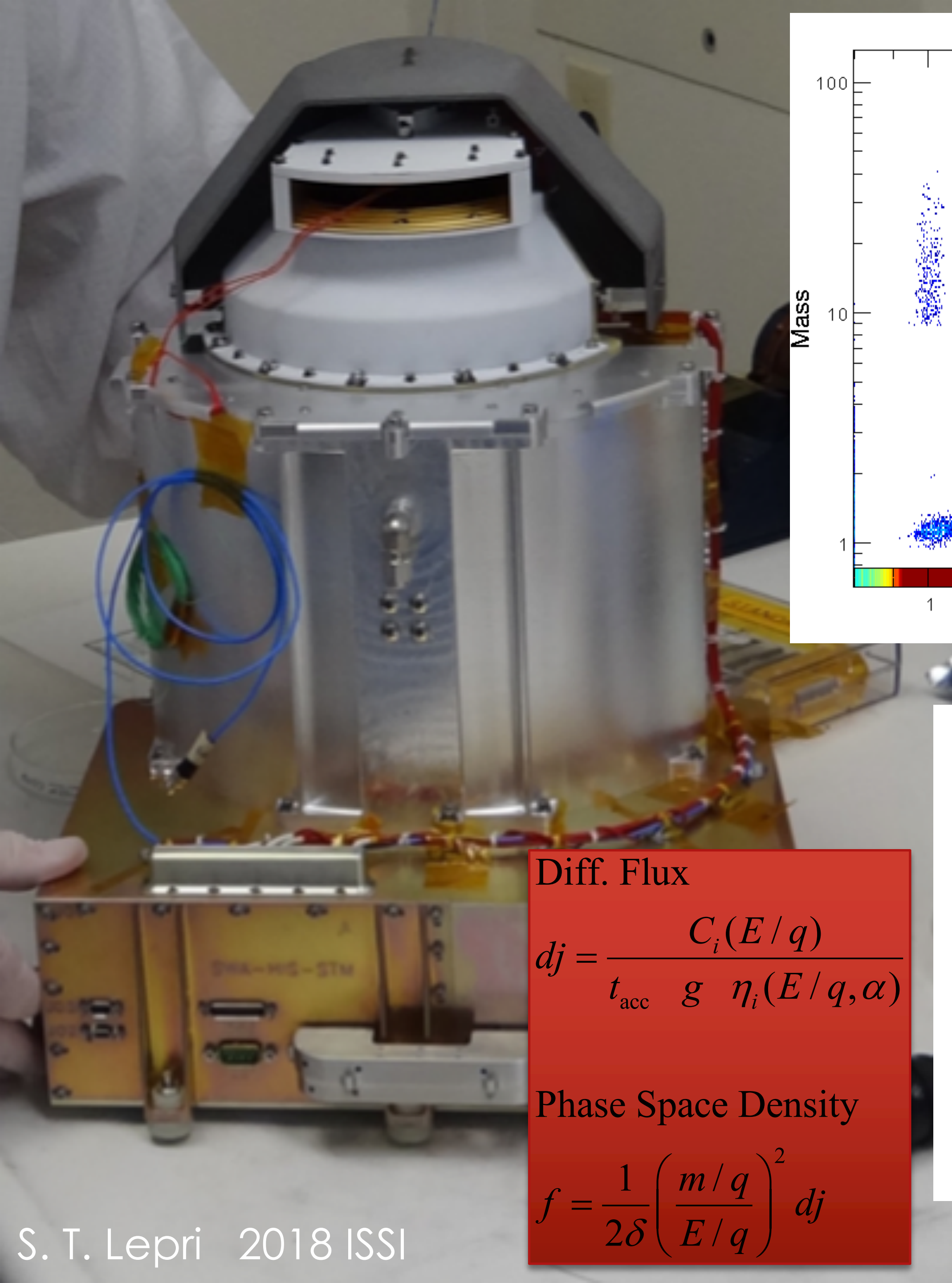

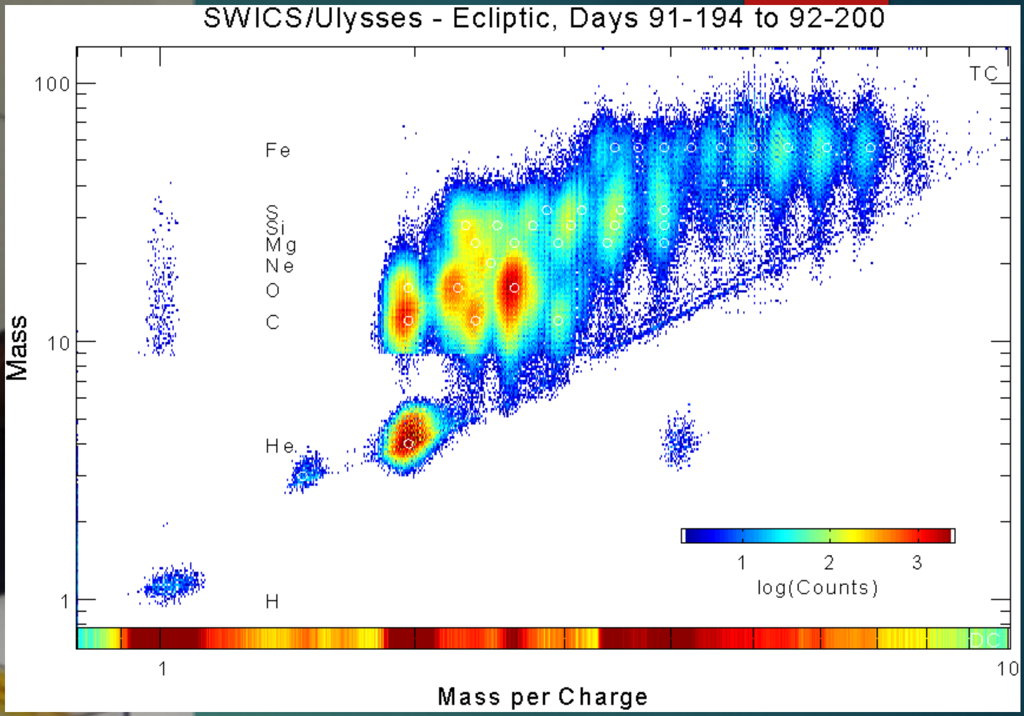

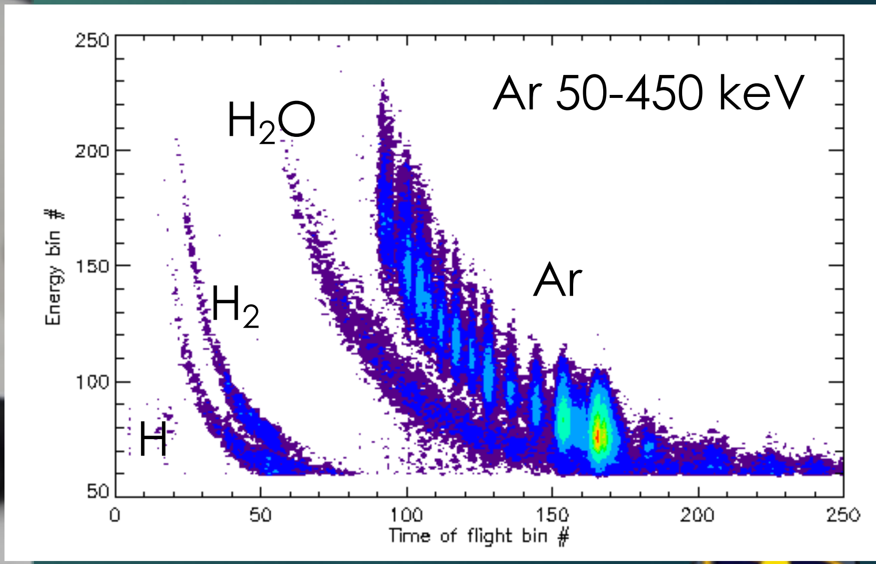

Diff. Flux

$$dj = \frac{C_i(E/q)}{t_{\mathrm{acc}} \quad g \quad \eta_i(E/q,\alpha)}$$

Phase Space Density

$$f = \frac{1}{2\delta}\left(\frac{m/q}{E/q}\right)^2 dj$$

New Science Enabled By HIS

- Radial evolution of solar wind features including SIRs, CMEs, shocks; e.g. sharpening of boundaries
- Higher resolution of small scale structures in the solar wind
- 3D distributions allow examination of temperature anisotropies, heating

Connecting Remote and In Situ Measurements

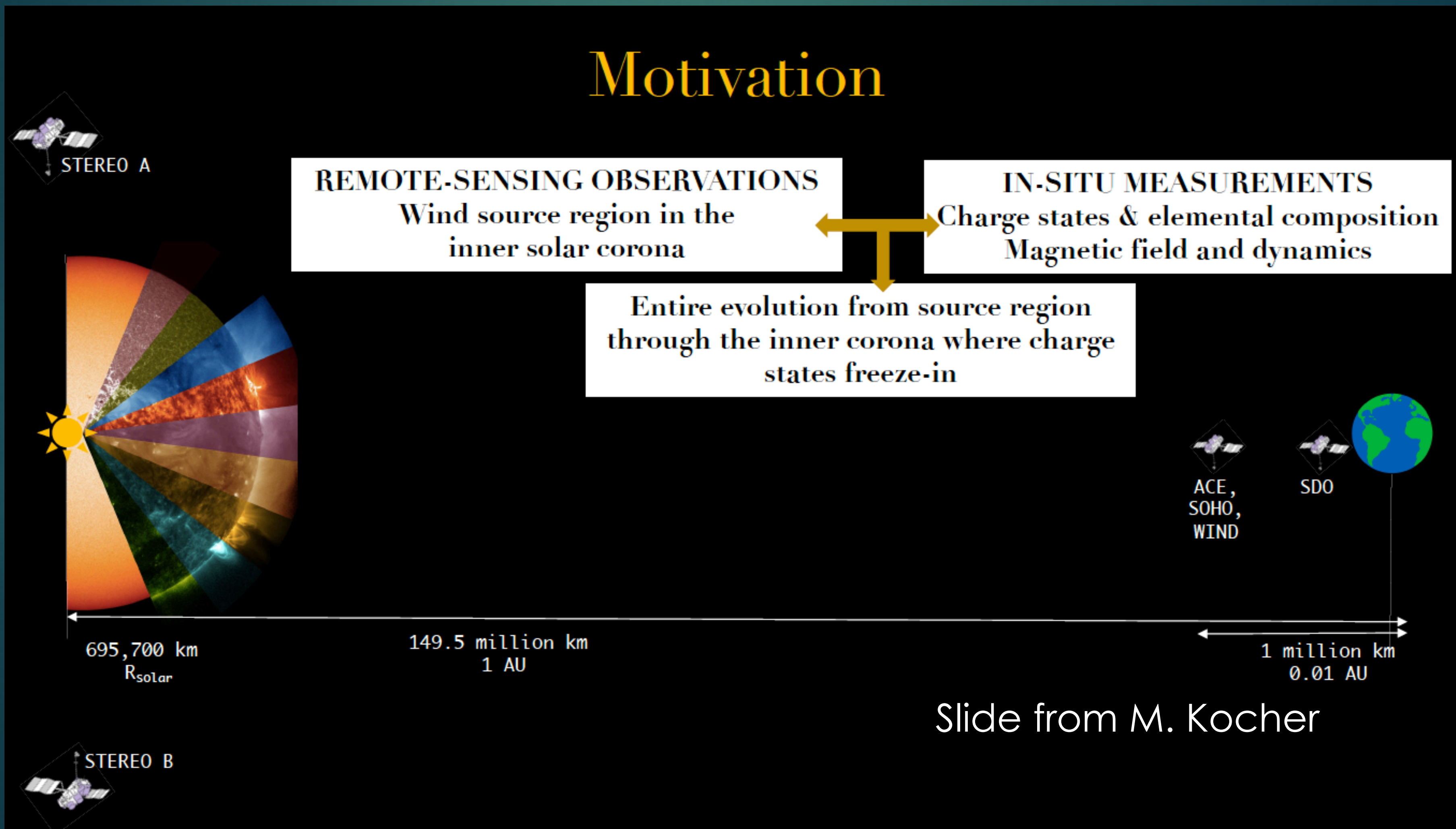

Solar Orbiter/SPICE

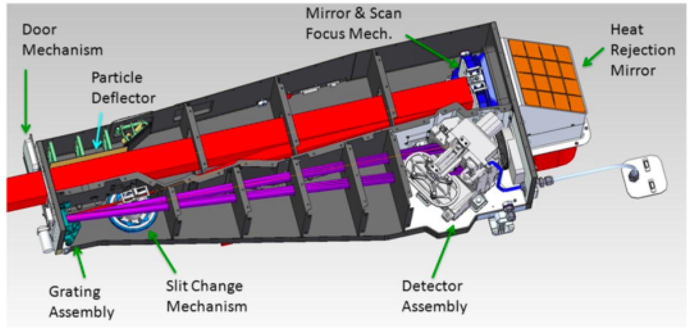

Figure 1. SPICE Optics Unit with major subsystems identified.

- Imaging spectrometer operating in EUV
- Measurements focus on investigating the outflow source regions and processes, linking the Sun to the Heliosphere.
- Covers 3+ orders of magnitude of plasma termperatures.
- Together SPICES and HIS will examine FIP fractionation and M/Q dependent processes at the Sun and in the heliosphere.

Fludra et al. (2013)

Table 1. SPICE line list

Ion	Wavelength (Å)	Log T (K)	FIP (eV)	M/q
H I Ly β	1025	4.0	13.6	---
C II	1036	4.3	11.3	12.0
C III	977	4.5	11.3	6.0
O IV	787.7	5.2	13.6	5.3
O V	760	5.4	13.6	4.0
O VI	1032	5.5	13.6	3.2
O VI	1037	5.5	13.6	3.2
S V	786.5	5.2	10.36	8.0
Ne VI	1005	5.5	21.6	4.0
Ne VII	973	5.6	21.6	3.3
Ne VIII	770	5.8	21.6	2.8
Mg VIII	772	5.9	7.7	3.4
Mg IX	706	6.0	7.7	3.0
Mg XI	997	6.2	7.7	2.4
Si VII	1049	5.6	8.1	4.8
Si XII	521 (2nd)	6.5	8.1	2.6
Fe X	1028	6.0	7.9	6.2
Fe XVIII	975	6.9	7.9	3.3
Fe XX	721	7.0	7.9	2.9
Auxiliary lines:				
Ne VIII	780	5.8	21.6	2.8
Si XII	499 (2nd)	6.5	8.1	2.6